microbial cell

Research Report

www.microbialcell.com

Direct detection of stringent alarmones (pp)pGpp using malachite green

Muriel Schicketanz[1], Magdalena Petrová[2], Dominik Rejman[2], Margherita Sosio[3], Stefano Donadio[3] and Yong Everett Zhang[1,*]

[1]Department of Biology, University of Copenhagen, DK2200, Copenhagen, Denmark. [2]Institute of Organic Chemistry and Biochemistry, Czech Academy of Sciences v.v.i, Prague, Czech Republic. [3]NAICONS Srl, 20139, Milan, Italy

*Corresponding Author:
Yong Everett Zhang, Department of Biology, University of Copenhagen, DK-2200 Copenhagen, Denmark; E-mail: yong.zhang@bio.ku.dk

ABSTRACT The alarmone (p)ppGpp serves as the signalling molecule for the bacterial universal stringent response and plays a crucial role in bacterial virulence, persistence, and stress adaptation. Consequently, there is a significant focus on developing new drugs that target and modulate the levels of (p)ppGpp as a potential strategy for controlling bacterial infections. However, despite the availability of various methods for detecting (p)ppGpp, a simple and straightforward detection method is needed. In this study, we demonstrated that malachite green, a well-established compound used for phosphate detection, can directly detect (p)ppGpp and its analogues esp., pGpp. By utilizing malachite green, we identified three new inhibitors of the hydrolase activity of SpoT, one of the two RelA-SpoT homolog (RSH) proteins responsible for making and hydrolyzing (p)ppGpp in *Escherichia coli*. These findings highlight the convenience and practicality of malachite green, which can be widely employed in high-throughput studies to investigate (pp)pGpp *in vitro* and discover novel regulators of RSH proteins.

doi: 10.15698/mic2024.08.834
Received originally: 24. 06. 2024;
in revised form: 05. 07. 2024,
Accepted: 08. 07. 2024
Published: 05. 08. 2024

Keywords: pppGpp, ppGpp, pGpp, SpoT, malachite green, thermorubin

Abbreviations:
HYD - hydrolase,
MG - malachite green,
Pi - orthophosphate,
ppGpp - guanosine-3′,5′-bisdiphosphate,
PPi - pyrophosphate,
pppGpp - guanosine-5′-triphosphate-3′-diphosphate,
RSH - RelA-SpoT homolog,
SYN - synthetase.

INTRODUCTION

First discovered in 1969 by Cashel and Gallant as spots appearing on autoradiograms from amino acid-starved *Escherichia coli* cells [1], the universal stringent response alarmone guanosine-3′,5′-bisdiphosphate (ppGpp) and guanosine-5′-triphosphate-3′-diphosphate (pppGpp) (collectively as (p)ppGpp) is well known for its importance in bacterial virulence, and tolerance and persistence to antibiotics [2–5]. Various stress conditions are now known to induce the production of (p)ppGpp, which affect bacterial global transcription, translation, and metabolism via its numerous target proteins [6, 7] to redistribute resources and, thus, survive the fluctuating environments [8, 9]. Elevated levels of (p)ppGpp are associated with antibiotic persistence, where bacteria enter a dormant state, leading to recurring and recalcitrant infections, and thereby occurrence of antibiotic resistance mutations [5, 10, 11]. Thus, targeting the stringent response is a promising strategy to combat bacterial antibiotic persistence and resistance [5].

The (p)ppGpp levels are regulated by the RelA-SpoT homologue (RSH) family proteins [12]. RelA in *E. coli* has only the synthetase (SYN) activity, producing ppGpp and pppGpp by transferring the pyrophosphate (PPi) of ATP to GDP and GTP, respectively [1, 13]. Whereas, SpoT has a weak SYN activity but a strong hydrolase (HYD) activity, degrading ppGpp and pppGpp in the presence of the co-factor Mn^{2+} [14–16]. Given the prominent role of RelA in producing (p)ppGpp, previous attempts have focused on inhibiting the SYN activity of RelA, such as the well-known example of relacin, which inhibits the SYN activity of RelA [17, 18]. Other similar molecules [17, 19] include the peptide 1018 that disperse biofilm by preventing the accumulation of (p)ppGpp [19] and a lead compound X9 targeting *Mycobacterium tuberculosis* Rel_{mtb} [20].

Despite the strong SYN activity of RelA, in many bacteria SpoT, instead of RelA, is more important for persistence [10, 21] and virulence [2, 22]. The HYD activity of SpoT is also essential to dynamically regulate intracellular levels of (p)ppGpp, as the key modulator of bacterial physiological changes in response to fluctuating environments. Consistently, deletion of *spoT* gene is impossible while *relA* is present [6], likely due to the uncontrolled production of (p)ppGpp, resulting in cell toxicity. Targeting the SpoT HYD activity is thus also promising.

Nevertheless, there are no reports about SpoT inhibitors. The lack of such reports may be due to the difficulty in purifying a stable full-length recombinant SpoT protein [4].

Another difficulty is the lack of a simple, accessible detection method of (p)ppGpp. The current methods used for detecting (p)ppGpp include the thin layer chromatography [1], radioimmunoassay [23], enzyme coupled reactions [24] or HPLC [25], which required three days to analyse 50 samples, being very time-consuming. Further, a fluorescent detection method for ppGpp, via the use of Eu^{3+} ion-functionalised fluorescent molybdenum sulfide quantum dots test paper, requires specific synthesis method, instrument and expertise [26]. A recent colourimetric method requires less preparation time as it utilises the redox reaction occurring between a Fenton-like reagent and 2,20-azino-bis-(3-ethylbenzthiazoline-6-sulfonic) acid [27]; however, PPi, which is the product of the SpoT HYD reaction, is also detected by this method.

In this study, we demonstrate the surprising discovery of a commercially available, low-cost malachite green (MG) detection kit, originally designed for orthophosphate (Pi) detection [28], for detecting (p)ppGpp and its analogues, especially pGpp [29]. We further developed a simple method utilizing MG to analyze the HYD activity of *E. coli* SpoT and show that SpoT can hydrolyze pGpp, pGp, and ppGp besides (p)ppGpp. Additionally, we screened both an in-house and commercial library of chemicals and identified the antibiotic thermorubin and two (p)ppGpp analogues DR-5839A and DR-6459 as novel inhibitors of the SpoT HYD activity. This study thus provides a very useful tool for the study of (p)ppGpp, pGpp and potential antimicrobial research targeting the RSH proteins.

RESULTS

Malachite green directly detects pppGpp, ppGpp and their analogs

To find a simple and suitable method for quantifying the SpoT HYD reaction, we suspected that both PPi and Pi may be produced by SpoT. The orthophosphate can be readily detected by the commercial MG (SIGMA-Aldrich, MAK307). To test, we purified a SpoT protein with a N-terminal Histidine-MBP-SUMO tag and a E319Q mutation. The SpoT E319Q mutation is expected to inactivate the SYN activity of SpoT (hereafter SYN_{off}) [30], avoiding its confounding effect on the HYD reaction. We then started two parallel SpoT HYD reactions with ppGpp, one with an active SpoT protein and the other with a heat inactivated SpoT as the negative control (see Material and Method for details). After 90 minutes' reaction, we added the MG detection mix to stop the reaction and detect the produced orthophosphates by spectrophotometric reading at 620 nm. Surprisingly, instead of an expected higher A_{620nm} value of the experimental group versus the negative control, the reverse was observed (Figure 1A). We thus suspected that either no Pi was produced and/or that ppGpp was detected by MG directly.

To discriminate, we mixed equal amount (35.6 μM) of pppGpp, ppGpp and their analogues, plus other relevant nucleotides directly with MG (Figure 1B). We found that, the highest A_{620nm} read was generated by pppGpp, followed by ppGpp, which is slightly higher than P_i. As stated in the manufacturer's manual, GTP had a slightly higher read compared to the buffer control. Interestingly, the (p)ppGpp analogues, pGpp, ppGp and pGp, were also detected, and pGpp gave a reading slightly lower than ppGpp/Pi but much higher than ppGp. pGp gave similar low readings as GTP, and GDP and PP_i were not significantly detected. These data demonstrate that the (p)ppGpp, pGpp, and ppGp can be detected by MG directly. Furthermore, the higher reading of pppGpp compared to ppGpp and higher reading of pGpp compared to ppGp, indicate that both the total number of Pi groups and the presence of an extra 5'- or 3'-phosphate are important for binding to MG. We further determined the detection limit of ppGpp to be about 2.94 μM (Figure 1C).

The malachite green kit can be used to assess the SpoT HYD activity

With the confirmed capacity of MG in detecting (p)ppGpp directly, we tested if the SpoT HYD activity can be assessed with MG. To this, we firstly performed the ppGpp hydrolysis reactions by using three different concentrations of SpoT SYN_{off} (50 nM, 100 nM, 200 nM). As a negative control (control-1, Figure 2A), heat inactivated SpoT SYN_{off} was used. Additionally, another control (control-2, Figure 2A) was included, which contained the reaction mix and the SpoT SYN_{off} protein but without ppGpp. As the anticipated products of the HYD reaction, GDP and PP_i, were shown not to give a significant signal (Figure 1C), a drop in A_{620nm} was expected. Indeed, this drop was observed (Figure 2A, 2B), for the samples containing active SpoT SYN_{off}, and that the greater the amount of SpoT used, the more pronounced the decrease in A_{620nm} became. On the other hand, the negative control-1 with heat inactivated SpoT gave highest A_{620nm} due to the non-hydrolyzed ppGpp and the control-2 gave lowest A_{620nm} due to the absence of ppGpp. These results confirmed that the reduction of A_{620nm} depends on the active SpoT SYN_{off} protein and its concentration, showing that ppGpp was detected by MG and that it can be used to assess the SpoT HYD activity *in vitro*.

PPi, instead of Pi, is the product of the SpoT hydrolase reaction

To have additional confirmation of the surprising ability of MG to detect (p)ppGpp, we tested if converting the product PP_i to Pi will increase A_{620nm} (Figure 2C). For this, we performed two parallel SpoT HYD reactions (S3, S4) for 60 min. After this, both reactions were stopped by heat inactivation, cooled down, and one reaction (S4) was added with pyrophosphatase (PPiase) for another 15 min before terminated and detected with MG reagent. The other reaction (S3) was added with both the PPiase and MG simultaneously. As controls, two other reactions (S1, S2) were performed. Both reactions contain the same setup as S3 and S4 but they contain heat inactivated SpoT SYN_{off} instead. Further, S1 was supplied with PPiase while S2 was not. Comparing the A_{620nm} readings, the similar readings of S1 and S2 indicate no residual PPi in the reaction mix. The lower A_{620nm} of S3 compared to S2 demonstrate the HYD activity of SpoT, while the much higher A_{620nm} of S4 compared to S3 demonstrates the further cleavage of PPi to Pi, which boosted the A_{620nm} significantly. Altogether, these tests show that PPi, instead of Pi, is the (main) product of SpoT hydrolytic reaction of ppGpp.

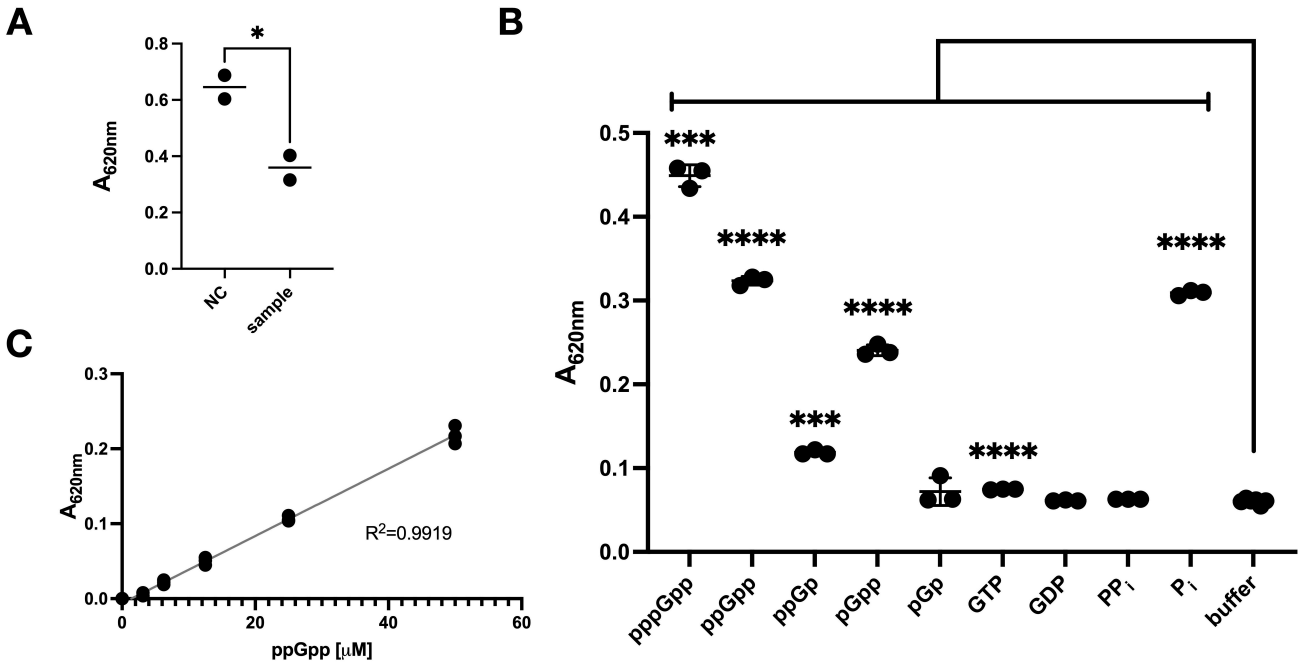

FIGURE 1 ● **Malachite green (MG) directly detects (p)ppGpp and its analogues.** (A) Detection of potential SpoT HYD reaction products with MG. ppGpp was incubated (90 min, room temperature) with purified SpoT protein with only the HYD activity, i.e., SYN_{off}. Afterwards, MG reagent was added to the reaction mixes and read at 620 nm (A_{620nm}). NC, sample: the two reactions with either heat inactivated or native SpoT SYN_{off} proteins, respectively. (B) Direct detection of the indicated chemicals by MG. The concentration of each compound was 35.6 μM (total volume 45 μl) before adding the MG detection mix. After 30 min incubation time, the absorbance at 620 nm (A_{620nm}) was assessed. (C) Standard curve of detecting ppGpp via the MG mix. The data shown are the mean ± SD of three technical replicates except for (A), which is of two replicates. The significance of unpaired t-test is indicated by the symbols $*$ (p-value < 0.05), $***$ (p-value < 0.001), and $****$ (p-value < 0.0001).

SpoT hydrolyses the 3′-phosphates of the (p)ppGpp analogues

Given the above result (Figure 2C) and the observations in Figure 1B, we were intrigued to test the substrate range of SpoT HYD and the detecting capacity of MG. For this, we performed the SpoT HYD assays towards pGpp, ppGp, and pGp (Figure 2D-F). As expected, SpoT SYN_{off} cleaves off the 3′-PPi of pGpp, resulting in GMP and thus a decreased reading (Figure 2D). The cleavage of 3′-Pi of both ppGp and pGp result in GDP/GMP and Pi, increasing the A_{620nm}, as seen in Figure 2E, 2F. Besides confirming the 3′-phosphate(s) HYD activity of SpoT, these results further validate that MG can detect (pp)pGp(p), despite with differential sensitivities.

Two ppGpp analogs, DR-5839A and DR-6459, inhibit SpoT HYD activity

The newly discovered detection ability of MG allowed us to design a facile screening method for chemicals that inhibit or accelerate the SpoT HYD activity. For this, we note that previously, (p)ppGpp analogues were found to inhibit the SYN activity of the SpoT homologue RelA, such as Relacin [18] or DR-4250 and DR-M014 [17]. We thus firstly tested the robustness of the MG method for screening in a 96-well plate, and the z′ value [31] was high at 0.644 (Supplementary Figure S1). Thus, we decided to screen a small number of (p)ppGpp analogues for potential effect on SpoT HYD activity. Out of the 30 ppGpp analogues (Supplementary Table S1), two (DR-5839A, DR-6459) displayed a clear inhibition of SpoT HYD activity (Figure 3A). Consistently, their chemical structures are highly similar (Figure 3B, 3C), with DR-5839A more similar as ppGpp, which is in line with its more pronounced inhibitory effect. However, none of them were significantly detected by MG directly (compare the two N.C. in Figure 3D, 3E and ppGpp in Figure 1B), possibly due to their chemical differences with ppGpp (see discussion below). The further incubation of SpoT SYN_{off} with either chemical alone did not generate a different reading of A_{620nm} (Figure 3D, 3E), suggesting that they cannot be hydrolysed by SpoT.

Thermorubin inhibits the SpoT HYD activity

Encouraged by the above small-scale screening, we decided to screen natural products affecting the SpoT HYD activity. To this end, we screened a collection of 60 known metabolites/antibiotics produced by actinomycetes (Supplementary Table S2). Remarkably, out of this screening, we identified thermorubin (Figure 3F) as a strong inhibitor of SpoT HYD activity. Thermorubin was discovered in 1964 as a natural product of *Thermoactinomyces antibioticus* [32] with antibacterial activities against Gram-negative and Gram-positive bacteria by inhibiting translation process [33–36]. Notably, the structurally similar tetracycline showed no effect on SpoT HYD activity (Supplementary Figure S2). Both tetracycline and thermorubin were dissolved in 10% DMSO. Together, these data suggest the specific binding and inhibition of SpoT by thermorubin. To compare the potency of thermorubin and DR-5839A, both the half-maximal inhibitory concentrations (IC_{50}) were determined. Thermorubin showed an IC_{50} of 7.43 ± 1.32 μM, while DR-5839A showed an approximately two-

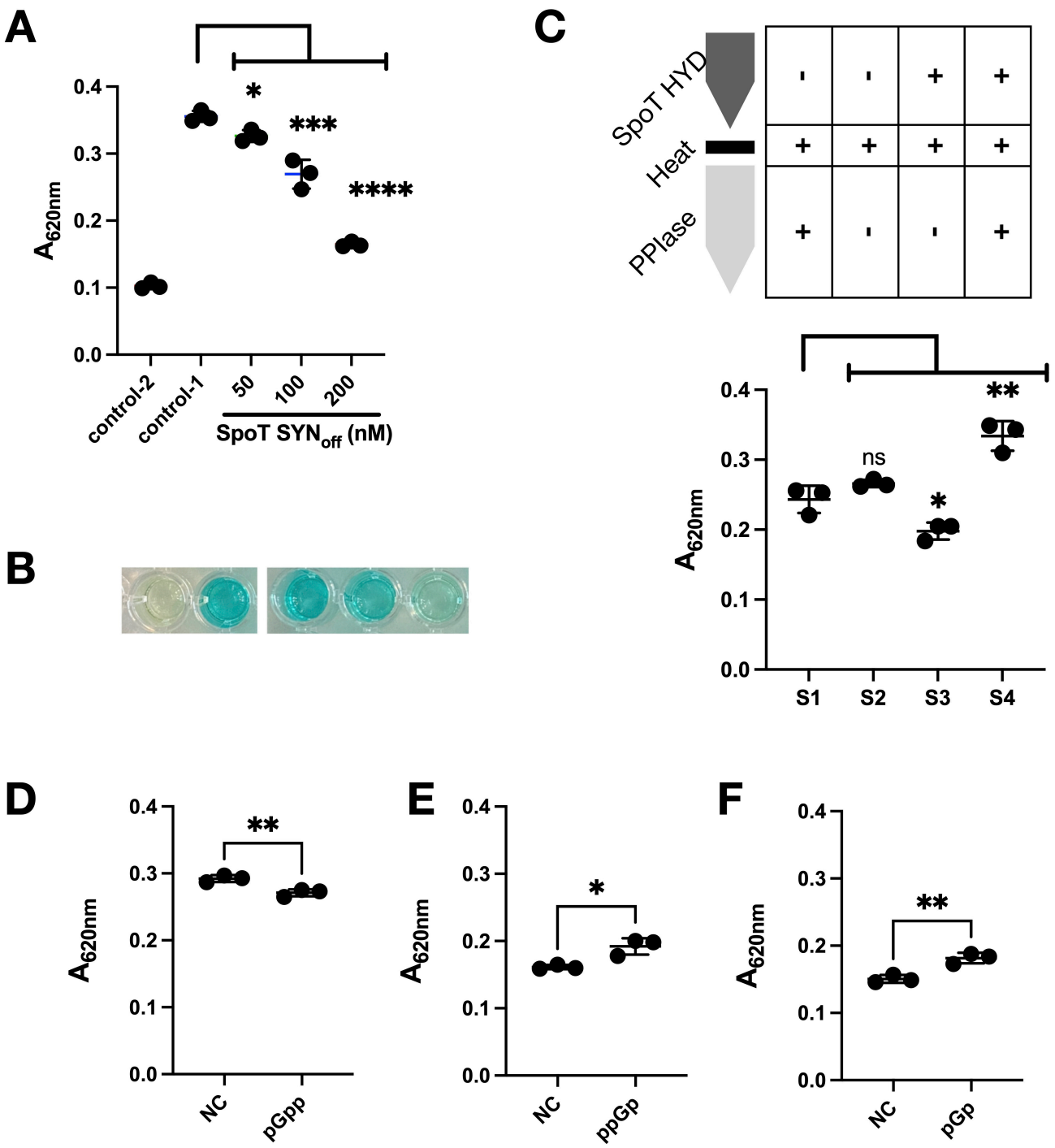

FiGURE 2 ● Assessing the hydrolase activity of SpoT by using MG. (A) SpoT concentration dependent reduction of MG detection signal (A_{620nm}). The SpoT reaction was given 90 minutes to occur before the MG detection mix was added. After 30 min incubation time, the absorbance (A_{620nm}) was read via a plate reader. Control-2 contained the reaction components without ppGpp but with SpoT SYN_{off} protein. Control-1 is identical with the SpoT SYN_{off} samples except that SpoT SYN_{off} was added just before the reaction was stopped with MG. (B) A representative picture of the sample wells of (A). (C) (top) The scheme of the reactions that were performed. PPiase = pyrophosphatase. (bottom) Absorbance at 620 nm for the reactions as indicated above. (D, E, F) Hydrolysis of (p)ppGpp analogues, pGpp, ppGp, and pGp (each at 35.6 μM) by SpoT SYN_{off} (100 nM, 90 min) and their detection by MG. NC, the SpoT HYD reactions were similarly set up, but MG working reagent was added immediately to stop the HYD reaction. The mean ± SD of three technical replicates were plotted. Unpaired t-test was performed and the significance is displayed by the symbols $*$ (p-value < 0.05), $**$ (p-value < 0.005).

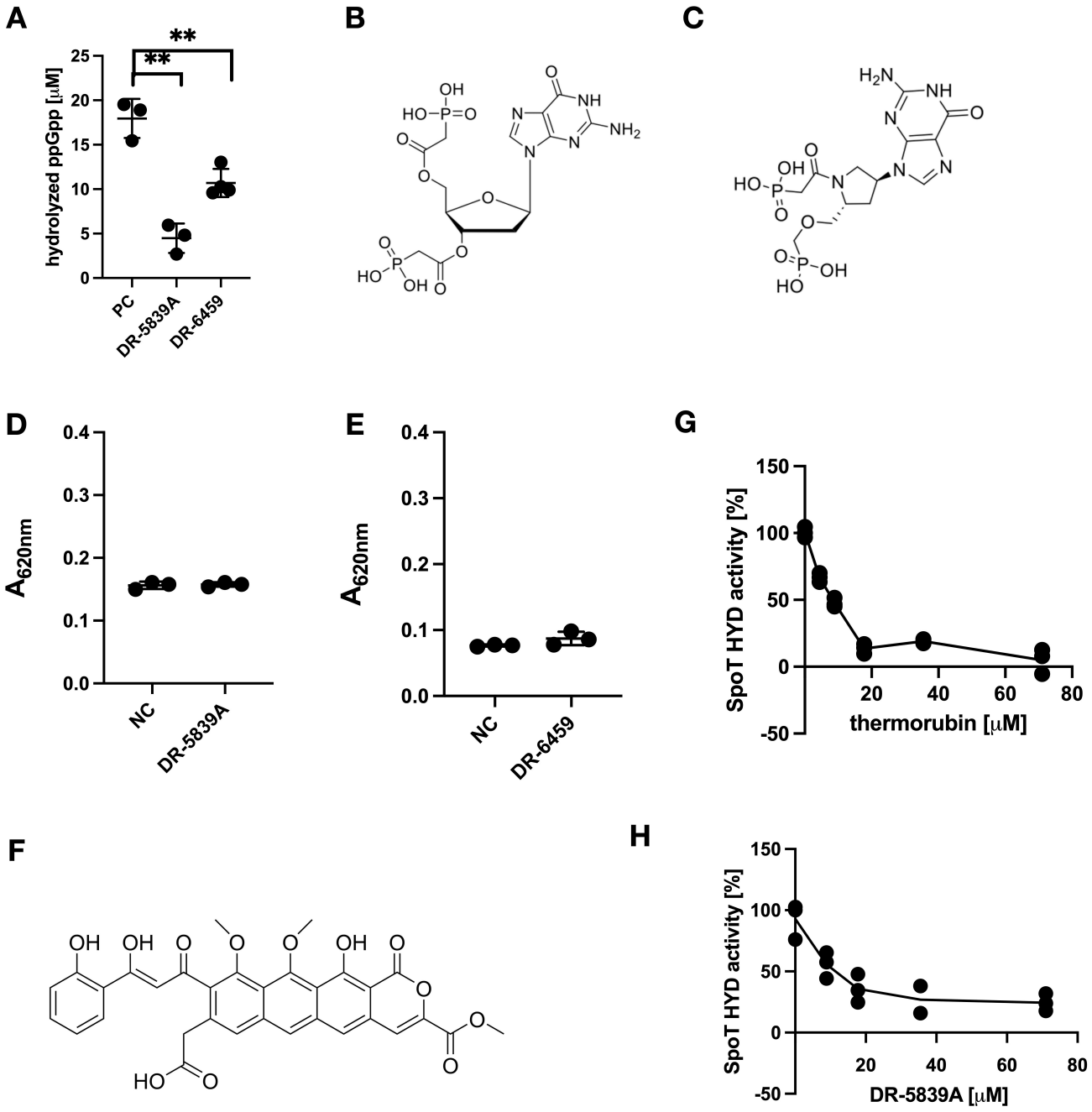

FIGURE 3 ● **Identification of novel chemical inhibitors of SpoT HYD activity.** (**A**) Hydrolysis of ppGpp (in μM) by SpoT SYN_{off} in the absence (PC) or presence of two ppGpp chemical analogues (DR-5839A, DR-6459). Unpaired t-test significance was displayed ($**$ p-value < 0.005). (**B, C**) Chemical structures of (**B**) DR-5839A and (**C**) DR-6459. (**D, E**) Test if DR-5839A and DR-6459 can be a substrate of SpoT HYD activity using MG. NC, the SpoT HYD reactions were similarly set up, but MG working reagent was added immediately to stop the HYD reaction. (**F**) Chemical structure of thermorubin. (**G, H**) IC_{50} measurement of both thermorubin (**G**) and DR-5839A (**H**). The activities shown in percentage were normalised to the sample without the respective chemical. The mean ± SD of three technical replicates were plotted.

times higher IC_{50} of 13.47 ± 3.73 μM (Figure 3G, 3H). Hence, thermorubin is a more potent inhibitor of SpoT HYD activity.

Given the higher *in vitro* inhibitory efficacy of thermorubin, we tested if thermorubin affects *E. coli* physiology. For this, we used the minimal medium (M9) supplemented with three amino acids, serine, methionine, and glycine (SMG) [37]. The presence of SMG applies a starvation condition that a high level of (p)ppGpp produced by RelA is required to support *E. coli* growth. Since thermorubin inhibits the HYD activity of SpoT, we suspect that it may allow the accumulation of ppGpp produced by SpoT, thus supporting cell growth of the Δ*relA spoTwt* strain in M9-SMG medium. As expected, Δ*relA spoTwt* is defective (Figure S3B) in growing in M9-SMG as compared to wild type (wt) *E. coli* (Figure S3A) and the double deletion strain Δ*relA* Δ*spoT* [38] cannot grow at all (Figure S3C). Further, addition of thermorubin did not enhance, but instead inhibited, the growth of Δ*relAspoTwt* in M9-SMG. Such an inhibitory effect was also observed for wt *E. coli* (Figure S3A). This could be due to the fact that thermorubin itself as an antibiotic directly binds to ribosome and inhibits translation process [33–35], thereby cell growth. Consistently, in a dose dependent manner thermorubin inhibits cell growth of all three *E. coli* strains, i.e., wt, Δ*relA spoTwt*, Δ*relA* Δ *spoT*, in the rich LB broth (Figure S4), wherein (p)ppGpp is dispensable for growth. In conclusion, the inhibitory effect of thermorubin on translation may have outweighed its ability to boost (p)ppGpp levels by inhibiting the SpoT HYD activity.

DISCUSSION

Simple and cost-effective (pp)pGpp detection method using MG

This study serendipitously discovered that MG (out of the MAK307 kit, Sigma-Aldrich) can directly detect (p)ppGpp *in vitro*. Several lines of evidence support this. 1) Heat inactivated SpoT produced higher A_{620nm} than active SpoT SYN_{off} protein (Figure 1A, 2C); and the more SpoT SYN_{off} proteins used, the lower the A_{620nm} became (Figure 2A). 2) (p)ppGpp and its analogues produced significant A_{620nm} readings when mixed up directly with MG, while GDP and PPi did not (Figure 1B). 3) Addition of PPiase restored the decreased A_{620nm} of the SpoT HYD reaction (Figure 2C), demonstrating that SpoT cleaves ppGpp to release PPi, which was hydrolyzed by PPiase, further increasing the A_{620nm} readings. 4) Cleavage of pGpp decreased the A_{620nm}, while cleavage of ppGp and pGp increased the A_{620nm}, demonstrating that SpoT cleaves the 3′ C-O bond, releasing either PPi or Pi depending on the substrates. Altogether, these data showed that MG directly detects (p)ppGpp, besides confirming the cleavage position of SpoT HYD activity on (p)ppGpp and its analogues pGpp, ppGp, and pGp.

The advantages of this MG method are clear to other methods as described above. MG is a well-developed chemical that is readily available, cheap and the detection reaction is fast (30 min). Therefore, MG could be used in large-scale high-throughput manner to screen for chemicals and proteins influencing the HYD (and SYN) activities of RSH proteins, as demonstrated in this study. However, limitations are also notable. Since MG does not discriminate Pi and (pp)pGpp, and the fact that biological samples without pre-clean up contain Pi and other potentially interfering molecules, one can only obtain at most the sum of all four molecules (i.e. Pi and (pp)pGpp) with MG, limiting its usage. Additionally, the ppGpp detection limit of MG is relatively high, despite an anticipated lower limit for pppGpp (Figure 1B). Nevertheless, we showed that MG could still be used for studying the HYD activity of SpoT, underscoring its usefulness in *in vitro* systematic studies. Lastly, MG could be used to study pGpp as well, a third stringent alarmone confirmed recently [29].

The (p)ppGpp detection mechanism by MG

Previously, MG was known to detect Pi by forming a complex with MG and molybdate, resulting in a shift in absorbance at 620 nm [28, 39]; however, the detection mechanism remains elusive. How does MG detect (p)ppGpp? Several features can be deduced from our data. pppGpp gave higher A_{620nm} than ppGpp, which is similar as Pi; however, ppGp gave much lower A_{620nm} than pGpp (Figure 1B). These data suggest the more of the total 3′ and 5′ Pi and particularly those at the 3′ position give higher A_{620nm} and thus detection by MG. However, PPi is not detected by MG, suggesting two different manners that how Pi and (p)ppGpp are detected by MG. Furthermore, both DR-5839A and DR-6459 gave lower A_{620nm} readings than ppGpp (Figure 3B-3E, 1B), suggesting that the 5′and 3′ Pi groups and their three-dimensional configurations also affect their detection by MG.

We note that, previously, the guanine-rich quadruplex could be detected by MG [40]. The potential mechanism involves pi-stacking between guanine and the triple phenyl ring of MG and maybe also electrostatic interactions. Therefore, the guanine ring of (p)ppGpp may pi-stack with MG, facilitating their interactions. Then, the 5′and 3′phosphates of (p)ppGpp may assume the similar position of free Pi, to be detected by MG. In support of this, both the 5′ and 3′ phosphates of (p)ppGpp are known to assume very flexible conformations [41], that may allow their detection of MG. Consistently, the one more 5′-gamma Pi of pppGpp produces higher A_{620nm} than ppGpp. We further suspect that MG may also detect other well-known nucleotide messengers such as AppppA [42] and ppApp [43, 44].

Novel inhibitors of SpoT HYD activity

Regardless the detection mechanism, MG provides a low-cost, fast, and simple spectrophotometric method for (p)ppGpp detection. MG can be used to study the HYD activity of SpoT *in vitro* as shown in this study (Figure 3). Via two screenings, we identified three inhibitors of the SpoT HYD activity, namely two (p)ppGpp analogues (DR-5839A and DR-6459) and the antibiotic thermorubin. Interestingly, tetracycline did not inhibit SpoT HYD despite its chemical similarity to thermorubin (Figure S2), confirming the specificity of thermorubin. Although the inhibitory manner of thermorubin remains elusive, both DR-5839A and DR-6459 potentially bind to the SpoT HYD active site, competitively inhibiting the HYD activity given the similar chemical structures to (p)ppGpp.

MATERIAL AND METHODS

Strains

Strains used in this study are listed in Table 1.

TABLE 1 ● Strains used in this study.

Strain	Genotype	
YZ37	MG1655 Wild type	Laboratory stock
YZ38	MG1655 Δ*relA*	Laboratory stock
YZ841	MG1655 Δ*relA* Δ *spoT*	[38]

Substrates and reagents

ppGpp and pppGpp were purchased from Jena Bioscience. pGpp was synthesized according to [45]. The other ppGpp analogues except for DR-6459 (synthesis described in the Supplementary Document S2) were synthesized as described in [17] (see detailed information in Supplementary document S1) and dissolved in 50 mM HEPES pH 8.0 with 150 mM NaCl. The PPiase and the PPi standard were taken from the EnzChek™ PPiAssay kit (ThermoFisher Scientific). The malachite green kit (MAK307) was purchased from Sigma-Aldrich, as well as all other remaining reagents. Tetracycline hydrochloride was purchased from Sigma-Aldrich. Thermorubin was provided by NAICONS Srl, purified from Thermoactinomyces antibioticus as previously described [32]. Both tetracycline and thermorubin were dissolved in 10% DMSO.

MG dye preparations

The MG detection mix was prepared as described in the manufacturer's manual (SIGMA-Aldrich, MAK307) by adding 1 volume of component B to 100 volumes of component A 30 min prior to use at room temperature (RT). For 45 μl reaction volume, 12 μl detection mix was added, and after 30 min incubation at RT, absorbance was measured at 620 nm.

SpoT SYN_{off} protein purification

E. coli Rosetta™ (DE3) (Novagen) was used in this study to express the SpoT SYN_{off} protein with a N-terminal Histidine-MBP-SUMO tag. Expression of spoT was induced at an optical density at 600 nm (OD_{600nm}) = 0.6 – 0.7 via the addition of 0.1 mM IPTG and subsequently shaking overnight at 20°C. The bacterial cells were collected and resuspended in 50 mM HEPES pH 8.0, 1 M NaCl, 10 mM imidazole, 5 mM beta-mercaptoethanol (BME) together with protease inhibitor (cOmplete™, Mini, EDTA-free Protease inhibitor cocktail). The cells were lysed by sonication (Amplitude 20%) and incubated with equilibrated Ni-NTA Agarose (Qiagen) and washed (50 mM HEPES pH 8.0, 1 M NaCl, 20 mM imidazole, 5 mM BME) before eluted (50 mM HEPES pH 8.0, 1 M NaCl, 500 mM imidazole, 5 mM BME) using a polypropylene chromatography column. The eluted protein was loaded on a size exclusion column Superdex 200 10/300 GL (GE Healthcare) equilibrated with 50 mM HEPES pH 8.0, 1 M NaCl, and 5% glycerol. Protein concentrations were assessed using a Bradford assay (Bio-Rad). The purified protein was frozen in liquid nitrogen and stored at -80°C.

SpoT HYD activity assay

All SpoT HYD reactions were carried out with a total reaction volume of 45 μl and a total reaction time of 90 min. The hydrolase activity reaction was performed at RT with 100 nM (or 200 nM and 50 nM when specified) SpoT SYN_{off} as the standard protein concentration. The reaction mix contained 50 mM HEPES pH 8.0, 150 mM NaCl, 2 mM BME, 0.2 mg/ml BSA, and 5 mM $MnCl_2$ and 35.6 μM ppGpp for the standard reaction. The reaction was started upon the addition of SpoT SYN_{off}. After 90 min, the reaction was stopped via the MG detection mix and the samples were assessed by absorbance at 620 nm.

Pyrophosphatase assay

After the SpoT HYD reaction is done and heat inactivated, 0.349 U Pyrophosphatase™ was added to the samples for 15 min incubation at RT, before terminated by adding the MG detection mix.

IC_{50} determination

The SpoT HYD activity assay was performed as described above, without or with the presence of respective concentrations of DR-5839A or thermorubin. The relative SpoT HYD activities were obtained by normalizing to that performed without either compound. The IC_{50} was calculated according to the 4-parameter logistic-model formula as described in [46].

Variation test of microtitre plate screening

The variation of the SpoT HYD assay was tested as described in the "SpoT HYD activity assay" except that the SpoT reaction time was 120 min and 84 positive controls (with reaction time 120 min) and 12 negative controls (with reaction time 0 min) were tested.

E. coli growth tests in M9-SMG medium

Overnight precultures were grown in Luria Bertani (LB) for 18 hours at 37°C, and cells were washed twice in 1x Phosphate Buffered Saline (PBS) and normalised in PBS before inoculated in M9-SMG medium to $OD_{600\,nm}$ = 0.005. The M9-SMG medium contains M9Glc minimal media (1x M9 salt, 1 mM $MgSO_4$, 0.2 % glucose, 0.1 mM $CaCl_2$, Thiamine (0.001 mg/1 ml)) and 100 μg/ml each of serine, glycine, and methionine [37]. In addition, the indicated concentration of thermorubin was added to the medium, and the growth was measured every 15 min for 24 hours in a plate reader (Biotek) at 37°C with double orbital agitation with a frequency of 548 cpm (2 mm).

Data analysis

Figures were generated via the software GraphPad Prism version 9.5.0, which was also used to perform unpaired t-test when indicated. At least three technical replicates were used for all reactions.

ACKNOWLEDGMENTS

The work is supported by a Novo Nordisk Foundation Project Grant (NNF19OC0058331) to Y.E.Z, the Project National Institute of Virology and Bacteriology (Programme EXCELES, ID Project N°. LX22NPO5103) funded by the European Union-Next

Generation EU to D.R., and the European Union's Horizon 2020 research and innovation programme under the Marie Skłodowska-Curie grant agreement (N° 801199) to M.S.

SUPPLEMENTAL MATERIAL

All supplemental data for this article are available online at www.microbialcell.com.

CONFLICT OF INTEREST

MSo and SD are shareholders of NAICONS, which owns the strain that produced the thermorubin used in this study.

COPYRIGHT

Please cite this article as: Muriel Schicketanz, Magdalena Petrová, Dominik Rejman, Margherita Sosio, Stefano Donadio, Yong Everett Zhang (**2024**). Direct detection of stringent alarmones (pp)pGpp using malachite green. **Microbial Cell** 11: 312-320. doi: 10.15698/mic2024.08.834

REFERENCES

1. Cashel M, Gallant J (**1969**). Two compounds implicated in the function of the RC gene of Escherichia coli. **Nature** 221 (5183): 838–841. doi:10.1038/221838a0

2. Dalebroux ZD, Svensson SL, Gaynor EC, Swanson MS (**2010**). ppGpp conjures bacterial virulence. **Microbiol Mol Biol Rev** 74 (2): 171–199. doi:10.1128/MMBR.00046-09

3. Harms A, Maisonneuve E, Gerdes K (**2016**). Mechanisms of bacterial persistence during stress and antibiotic exposure. **Science** 354 (6318): 4268–4268. doi:10.1126/science.aaf4268

4. Hauryliuk V, Atkinson GC, Murakami KS, Tenson T, Gerdes K (**2015**). Recent functional insights into the role of (p)ppGpp in bacterial physiology. **Nat Rev Microbiol** 13 (5): 298–309. doi:10.1038/nrmicro3448

5. Pacios O, Blasco L, Bleriot I, Fernandez-Garcia L, Ambroa A, López M, Bou G, Cantón R, Garcia-Contreras R, Wood TK, Tomás M (**2020**). and Its Role in Bacterial Persistence: New Challenges. **Antimicrob Agents Ch** 64 (10): ppGpp–ppGpp. doi:10.1128/AAC.01283-20

6. Zhang Y, Zborníková E, Rejman D, Gerdes K (**2018**). Novel (p)ppGpp Binding and Metabolizing Proteins of Escherichia coli. **mBio** 9 (2): 2188–2205. doi:10.1128/mBio.02188-17

7. Wang B, Dai P, Ding D, Rosario AD, Grant RA, Pentelute BL, Laub MT (**2019**). Affinity-based capture and identification of protein effectors of the growth regulator ppGpp. **Nat Chem Biol** 15 (2): 141–150. doi:10.1038/s41589-018-0183-4

8. Traxler MF, Summers SM, Nguyen HT, Zacharia VM, Smith JT, Conway T (**2008**). The global, ppGpp-mediated stringent response to amino acid starvation in Escherichia coli. **Mol Microbiol** 68 (5): 1128–1148. doi:10.1111/j.1365-2958.2008.06229.x

9. Dalebroux ZD, Swanson MS (**2012**). ppGpp: magic beyond RNA polymerase. **Nat Rev Microbiol** 10 (3): 203–212. doi:10.1038/nrmicro2720

10. Korch SB, Henderson TA, Hill TM (**2003**). Characterization of the hipA7 allele of Escherichia coli and evidence that high persistence is governed by (p)ppGpp synthesis. **Mol Microbiol** 50 (4): 1199–1213. doi:10.1046/j.1365-2958.2003.03779.x

11. Rodionov DG, Ishiguro EE (**1995**). Direct Correlation between Overproduction of Guanosine 3',5'-Bispyrophosphate (Ppgpp) and Penicillin Tolerance in Escherichia-Coli. **J Bacteriol** 177 (15): 4224–4229. doi:10.1128/jb.177.15.4224-4229.1995

12. Atkinson GC, Tenson T, Hauryliuk V (**2011**). The RelA/SpoT homolog (RSH) superfamily: distribution and functional evolution of ppGpp synthetases and hydrolases across the tree of life. **PLoS One** 6 (8): 23,479–23,479. doi:10.1371/journal.pone.0023479

13. Sy J, Lipmann F (**1973**). Identification of the synthesis of guanosine tetraphosphate (MS I) as insertion of a pyrophosphoryl group into the 3'-position in guanosine 5'-diphosphate. **Proc Natl Acad Sci U S A** 70 (2): 306–309. doi:10.1073/pnas.70.2.306

14. An G, Justesen J, Watson RJ, Friesen JD (**1979**). Cloning the spoT gene of Escherichia coli: identification of the spoT gene product. **J Bacteriol** 137 (3): 1100–1110. doi:10.1128/jb.137.3.1100-1110.1979

15. Xiao H, Kalman M, Ikehara K, Zemel S, Glaser G, Cashel M (**1991**). Residual guanosine 3',5'-bispyrophosphate synthetic activity of relA null mutants can be eliminated by spoT null mutations. **J Biol Chem** 266 (9): 5980–5990. doi:10.1016/s0021-9258(19)67694-5

16. Heinemeyer EA, Geis M, Richter D (**1978**). Degradation of Guanosine 3'-diphosphate 5'-diphosphate in vitro by the spoT Gene Product of Escherichia coli. **Eur J Biochem** 89 (1): 125–131. doi:10.1111/j.1432-1033.1978.tb20904.x

17. Beljantseva J, Kudrin P, S J, Ehn M, Pohl R, Varik V, Tozawa Y, Shingler V, Tenson T, Rejman D, Hauryliuk V (**2017**). Molecular mutagenesis of ppGpp: turning a RelA activator into an inhibitor. **Sci Rep** 7: 41,839–41,839. doi:10.1038/srep41839

18. Wexselblatt E, Oppenheimer-Shaanan Y, Kaspy I, London N, Schueler-Furman O, Yavin E, Glaser G, Katzhendler J, Ben-Yehuda S (**2012**). Relacin, a novel antibacterial agent targeting the Stringent Response. **PLoS Pathog** 8 (9): 1002,925–1002,925. doi:10.1371/journal.ppat.1002925

19. Dlc FN, Reffuveille F, Haney EF, Straus SK, Hancock REW (**2014**). Broad-Spectrum Anti-biofilm Peptide That Targets a Cellular Stress Response. **PLOS Pathogens** 10 (5): 1004,152–1004,152. doi:10.1371/journal.ppat.1004152

20. Dutta NK, Klinkenberg LG, Vazquez MJ, Segura-Carro D, Colmenarejo G, Ramon F, Rodriguez-Miquel B, Mata-Cantero L, Francisco EPD, Chuang YM, Rubin H, Lee JJ, Eoh H, Bader JS, Perez-Herran E, Mendoza-Losana A, Karakousis PC (**2019**). Inhibiting the stringent response blocks entry into quiescence and reduces persistence. **Sci Adv** 5 (3). doi:10.1126/sciadv.aav2104

21. Viducic D, Ono T, Murakami K, Susilowati H, Kayama S, Hirota K, Miyake Y (**2006**). Functional Analysis of spoT, relA and dksA Genes on Quinolone Tolerance in Pseudomonas aeruginosa under Nongrowing Condition. **Microbiol Immunol** 50 (4): 349–357. doi:10.1111/j.1348-0421.2006.tb03793.x

22. Sun W, Roland KL, Branger CG, Kuang X, Iii RC (**2009**). The Role of relA and spoT in Yersinia pestis KIM5+ Pathogenicity. **PLOS ONE** 4 (8): 6720–6720. doi:10.1371/journal.pone.0006720

23. Riesenberg D (**1985**). A radioimmunoassay for (p)ppGpp and its application to Streptomyces hygroscopicus. **J Basic Microbiol** 25 (2): 127–140. doi:10.1002/jobm.3620250209

24. Potrykus K, Thomas NE, Bruhn-Olszewska B, Sobala M, Dylewski M, James T, Cashel M (**2020**). Estimates of RelSeq, Mesh1, and SAHMex Hydrolysis of (p)ppGpp and (p)ppApp by Thin Layer Chromatography and NADP/NADH Coupled Assays. **Front Microbiol** 11: 581,271–581,271. doi:10.3389/fmicb.2020.581271

25. Varik V, Oliveira S, Hauryliuk V, Tenson T (**2017**). HPLC-based quantification of bacterial housekeeping nucleotides and alarmone messengers ppGpp and pppGpp. **Sci Rep** 7 (1): 11,022–11,022. doi:10.1038/s41598-017-10988-6

26. Rong M, Ye J, Chen B, Wen Y, Deng X, Liu ZQ (**2020**). Ratiometric fluorescence detection of stringent ppGpp using Eu-MoS2 QDs test paper. **Sensors and Actuators B: Chemical** 309: 127,807–127,807. doi:10.1016/j.snb.2020.127807

27. Zheng LL, Huang CZ (**2014**). Selective and sensitive colorimetric detection of stringent alarmone ppGpp with Fenton-like reagent. **Analyst** 139 (23): 6284–6289. doi:10.1039/c4an01632g

28. Itaya K, Ui M (**1966**). A new micromethod for the colorimetric determination of inorganic phosphate. **Clinica Chimica Acta** 14 (3): 361–366. doi:10.1016/0009-8981(66)90114-8

29. Yang J, Anderson BW, Turdiev A, Turdiev H, Stevenson DM, Amador-Noguez D, Lee VT, Wang JD (**2020**). The nucleotide pGpp acts as a third alarmone in Bacillus, with functions distinct from those of (p) ppGpp. **Nat Commun** 11 (1): 5388–5388. doi:10.1038/s41467-020-19166-1

30. Harinarayanan R, Murphy H, Cashel M (**2008**). Synthetic growth phenotypes of Escherichia coli lacking ppGpp and transketolase A (tktA) are due to ppGpp-mediated transcriptional regulation of tktB. **Mol Microbiol** 69 (4): 882–894. doi:10.1111/j.1365-2958.2008.06317.x

31. Jh Z, Td C, Kr O (**1999**). A Simple Statistical Parameter for Use in Evaluation and Validation of High Throughput Screening Assays. **J Biomol Screen** 4 (2): 67–73. doi:10.1177/108705719900400206

32. Craveri R, Coronelli C, Pagani H, Sensi P (**1964**). Thermorubin, a New Antibiotic from a Thermoactinomycete. **Clin Med Winnetka, Ill** 71 (3): 15446,134–15446,134

33. Parajuli NP, Emmerich A, Mandava CS, Pavlov MY, Sanyal S (**2023**). Antibiotic thermorubin tethers ribosomal subunits and impedes A-site interactions to perturb protein synthesis in bacteria. **Nat Commun** 14 (1): 918–918. doi:10.1038/s41467-023-36528-7

34. Lin FL, Wishnia A (**1982**). The protein synthesis inhibitor thermorubin. 1. Nature of the thermorubin-ribosome complex. **Biochemistry** 21 (3): 477–483. doi:10.1021/bi00532a010

35. Pirali G, Somma S, Lancini GC, Sala F (**1974**). Inhibition of peptide chain initiation in Escherichia coli by thermorubin. **Biochim Biophys Acta** 366 (3): 310–318. doi:10.1016/0005-2787(74)90291-3

36. Cavalleri B, Turconi M, Pallanza R (**1985**). Synthesis and antibacterial activity of some derivatives of the antibiotic thermorubin. **J Antibiot** 38 (12): 1752–1760. doi:10.7164/antibiotics.38.1752

37. Uzan M, Danchin A (**1976**). A rapid test for the rel A mutation in E. coli. **Biochem Biophys Res Commun** 69 (3): 90,939–90,945. doi:10.1016/0006-291x(76)90939-6

38. Grucela PK, Zhang YE (**2023**). Basal level of ppGpp coordinates Escherichia coli cell heterogeneity and ampicillin resistance and persistence. **Microbial Cell** 10 (11): 248–260. doi:10.15698/mic2023.11.808

39. Baykov AA, Evtushenko OA, Avaeva SM (**1988**). A malachite green procedure for orthophosphate determination and its use in alkaline phosphatase-based enzyme immunoassay. **Anal Biochem** 171 (2): 266–270. doi:10.1016/0003-2697(88)90484-8

40. Bhasikuttan AC, Mohanty J, Pal H (**2007**). Interaction of malachite green with guanine-rich single-stranded DNA: preferential binding to a G-quadruplex. **Angew Chem Int Edit** 46 (48): 9305–9307. doi:10.1002/anie.200703251

41. Steinchen W, Bange G (**2016**). The magic dance of the alarmones (p). **Mol Microbiol** 101 (4): 531–544. doi:10.1111/mmi.13412

42. Giammarinaro PI, Young M, Steinchen W, Mais CN, Hochberg G, Yang J, Stevenson DM, Amador-Noguez D, Paulus A, Wang JD, Bange G (**2022**). Diadenosine tetraphosphate regulates biosynthesis of GTP in Bacillus subtilis. **Nat Microbiol** 7 (9): 1442–1452. doi:10.1038/s41564-022-01193-x

43. Fung DK, Yang J, Stevenson DM, Amador-Noguez D, Wang JD (**2020**). Small Alarmone Synthetase SasA Expression Leads to Concomitant Accumulation of pGpp, ppApp, and AppppA in Bacillus subtilis. **Front Microbiol** 11: 2083–2083. doi:10.3389/fmicb.2020.02083

44. Ahmad S, Wang B, Walker MD, Tran HR, Stogios PJ, Savchenko A, Grant RA, Mcarthur AG, Laub MT, Whitney JC (**2019**). An interbacterial toxin inhibits target cell growth by synthesizing (p)ppApp. **Nature** 575 (7784): 674–678. doi:10.1038/s41586-019-1735-9

45. Horvatek P, Salzer A, Hanna A, Gratani FL, Keinhörster D, Korn N, Borisova M, Mayer C, Rejman D, Mäder U, Wolz C (**2020**). Inducible expression of (pp)pGpp synthetases in Staphylococcus aureus is associated with activation of stress response genes. **Plos Genetics** 16 (12): 1009,282–1009,282. doi:10.1371/journal.pgen.1009282

46. Sebaugh JL (**2011**). Guidelines for accurate EC50/IC50 estimation. **Pharmaceutical Statistics** 10 (2): 128–134. doi:10.1002/pst.426